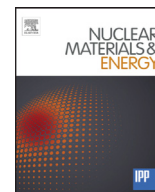




ELSEVIER

Contents lists available at ScienceDirect

Nuclear Materials and Energy

journal homepage: www.elsevier.com/locate/nme

LIBS experiments for quantitative detection of retained fuel

F. Colao^{a,*}, S. Almagia^a, L. Caneve^a, G. Maddaluno^a, T. Fornal^b, P. Gasior^b, M. Kubkowska^b, M. Rosinski^b^aENEA, Italian National Agency for New Technologies, Energy and sustainable Economic Development, C.R. Frascati, via Enrico Fermi, 44, Frascati, 00045, Italy^bIPPLM, Institute of Plasma Physics and Laser Microfusion, P.O. Box 49, Hery St. 23, Warsaw 00-908, Poland

ARTICLE INFO

Article history:

Received 7 October 2016

Revised 4 April 2017

Accepted 30 May 2017

Available online xxx

ABSTRACT

Laser Induced Breakdown Spectroscopy (LIBS) provides chemical information from atomic and ionic plasma emissions generated by laser vaporization of a sample. At the ENEA research center, in collaboration with IPPLM, an equipment has been set up to qualitatively and quantitatively determine the chemical composition of impurities deposited on Plasma Facing Components (PFC). The strength of the LIBS, for its capability of light elements detection, is fully exploited to determine the deuterium content since this element can be considered as the best choice proxy for tritium; the latter being is of great importance in assessing safe conditions to assure the continuous operation in nuclear fusion tokamak.

Here we present the results of the Double Pulse LIBS (DP-LIBS) probing of deuterated samples with the simultaneous optical detection by medium-resolution and high-resolution spectrometer. Deuterium emission at 656.1 nm has been detected then the elemental composition has been quantified by applying the Calibration Free (CF) approach. The obtained results demonstrate that the DP-LIBS technique combined with CF analysis is suitable for the quantitative determination of tritium content inside the PFCs of next fusion devices like ITER.

© 2017 Published by Elsevier Ltd.

This is an open access article under the CC BY-NC-ND license. (<http://creativecommons.org/licenses/by-nc-nd/4.0/>)

Introduction

The formation of co-deposited layers in fusion reactors is a main concern for the safety of the operation, since this formation involves fuel retention. Methods must be studied allowing for the by in situ and real time quantitative measurements of deuterium and tritium trapped on the metallic wall of next fusion devices like ITER. [1,2].

Among viable techniques, the ablation of ns pulsed laser and the analysis of plasma emissions sustained by excitation is one of the most promising. Indeed the process of laser ablation of metals is complex, since it depends on several factors including the material, the environmental parameters and the laser pulse excitation in terms of pulse energy, time duration, wavelength, and beam quality [3,4]. In order to obtain satisfactory quantitative analysis, especially in case of determination of trace elements, it is necessary a good understanding of the interaction of the sample with the laser [5]; also the phenomena associated with the laser ablation must be

carefully considered since the signal is proportional to the density of the emitting species and definitively to the ablated mass.

LIBS studies in vacuum [6,7] have shown that the multiphoton ionization provides the initial electrons and plays a very important role for the breakdown phenomenon; here the electron free path well exceed the plasma volume and the electron cascade is strongly depressed. The DP-LIBS plays in vacuum a crucial role; indeed provided that the interpulse delay is of the order of magnitude of the ratio between the plasma mean radius and the particles velocity, the first pulse substantially modifies the local density of particles facing the second laser pulse favoring the laser plasma interactions and increasing the ablated mass [8].

The typical laboratory plasmas are characterized by a predominance of the electron impact processes, while the radiative losses do have a negligible contribution to the plasma kinetics [9]. Moreover the possibility to define a suitable time window for the existence of a Local Thermodynamic Equilibrium (LTE) is currently accepted. Accordingly it is possible to define a local temperature T at each point in space in such a way that the plasma formed by atoms, ions and electrons, is uniquely described by means of the number density of electrons and one thermodynamic parameter, namely the temperature which is assumed to be the same for all

* Corresponding author.

E-mail address: francesco.colao@enea.it (F. Colao).<http://dx.doi.org/10.1016/j.nme.2017.05.010>2352-1791/© 2017 Published by Elsevier Ltd. This is an open access article under the CC BY-NC-ND license. (<http://creativecommons.org/licenses/by-nc-nd/4.0/>)

the species present in the plasma [10]. In LTE, the species density follows the Saha–Eggert relationship, while the ions and electrons energy distribution are described by Boltzmann and Maxwell respectively [11]. It is therefore possible to analytically model the atoms and ions populations, nevertheless their exact computation critically depend on the partition function, which requires the availability of a sufficiently complete set of atomic energy levels as well as an appropriate definition of the ionization potential lowering [10]. Finally once the plasma parameters are completely characterized, the analytical approaches like the Calibration Free and its variants allow for quantitative elemental determination of major elements, while the assessment of the attained accuracy for minor and trace elements still need for further studies [11].

The Double Pulse (DP) technique has been reported as a viable technique to enhance the LIBS signal in several experimental conditions including the atmospheric air pressure [21] and vacuum [22]. The mechanisms responsible of the signal enhancement are mainly related to the modifications in the environment produced by the first laser pulse, which create the optimal conditions for the laser target and laser plume interactions of the second laser pulse. Babushok et al. in [23] discuss various parameters which characterize both the processes in the target material and in the gas plasma plume. Mechanisms responsible for enhancement in nanosecond excitation DP-LIBS at atmospheric pressure are related to the changes in the environment surrounding the sample caused by the first laser pulse; consequently the second laser pulse undergoes to lower shielding and a better coupling with the target. On the other hand in DP-LIBS in vacuum the plasma induced by the first laser pulse expands almost freely in the absence of counterpressure of the ambient gas, with low density low plasma absorption, while the second laser pulse is effectively coupled with plasma.

Several attempts have been made to apply LIBS based techniques to the qualitative and quantitative determination of hydrogen and its isotopes content deposited on PFCs as well as to the in depth analysis [12–17].

In a collaboration work supported by EURATOM and carried out within the framework of the European Fusion Development Agreement several European laboratories led by Malaquias [12] firstly demonstrated the feasibility of quantitative determination of deuterium deposited on metallic sample by LIBS. In this work also an attempt to apply the Calibration Free method to deuterium codeposited Plasma Facing Components (PFC) in vacuum is presented for the first time.

Semerok et al. [13] applied the LIBS to the analysis of tungsten coated samples, discussing the feasibility of tritium inventory.

To obtain quantitative determination of retained fuel, Gierse et al. [14] made an experimental estimation of the photon efficiency for the Balmer α line of deuterium, resulting from laser ablation on amorphous hydrocarbon layers deposited on tungsten.

Piip et al. [15] analyzed in situ and post mortem deuterated samples, proposing a novel method for the elemental quantitative determination based on the normalization of LIBS data as a function of laser shot number.

Pribula et al. [16] used extended Saha–Boltzmann plot from neutral, singly and doubly ionized lines of tungsten at short delays up to several hundreds of nanoseconds for the evaluation of electron temperature as a mean to improve the quantitative elemental content determination by CF-LIBS method.

Several conditions must be fulfilled when using the LIBS spectrometry for quantitative analytical applications, whose main objective is to provide quantitative information with high accuracy and precision. In this case it is required that the ablated material has a composition similar to that of the sample under analysis; a simplifying condition is also obtained whenever the plasma is optically thin, since in this case the effect of self-absorption of the ra-

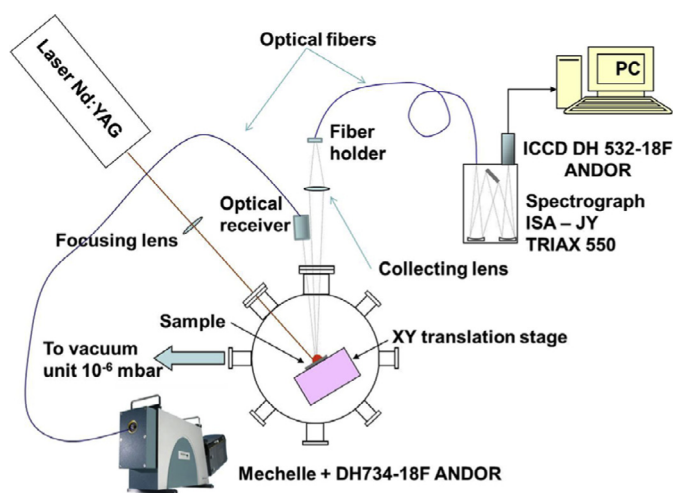


Fig. 1. LIBS setup.

diation emitted from the plasma itself is avoided [18]. The concentration of sample elemental constituents can be obtained by means of the calibration curve, i.e. a relationship between the response and the mass or concentration of the analyte in a given range. Quantitative analysis by means of calibration curves presents several drawbacks mainly related to the effect matrix [19]; in order to reduce the influence of the matrix, reference samples must be made with a composition similar to that of the unknown sample. On the other hand the technique requires the availability of reference samples with a wide range of concentration, encompassing that of the analyte in question. Finally a calibration curve is needed for each one of the elements under study. It is possible to overcome these problems by using standard-less calibration methods with special reference to the CF technique; moreover it is worth mention that the approaches devised for the quantitative determination of the minor constituents lead to accuracy of the order of 20%, which is well within the requirement put by fusion machines as for example ITER.

Experimental

The sample used for this work was prepared by coating a molybdenum substrate with a 1.5 μm thick tungsten layer. Successfully the sample was exposed to D_2 plasma in the Pilot-PSI device [20]. The plasma flow was about $16.9 \text{ mbar l s}^{-1}$, corresponding to $4.1 \times 10^{20} \text{ ions s}^{-1}$, the FWHM of the beam about 25 mm and the exposure time 910 s, on an implanted area of about 5 cm^2 . The surface density of impinging ions was $7.6 \times 10^{26} \text{ ions/m}^2$. The energy of the D ions was determined by the sample biasing and was 40 eV; the sample temperature during the implantation was between $200 \text{ }^\circ\text{C}$ and $300 \text{ }^\circ\text{C}$.

The main components of the used LIBS set up are shown in Fig. 1. Basic components of the experimental set-up are a twin laser, a focusing lens and a detection system to spectrally resolve the collected light; finally, a personal computer is used for signal processing and data storage.

The excitation source is a solid state laser system (TII LS-2131D from LOTIS LOT); the flash lamps independently pump two Nd:YAG rods each of them is capable to produce typical pulse widths of $9\text{--}12 \text{ ns}$ at the fundamental wavelength at 1064 nm. Two Q-switched independent resonators leave the user with a complete freedom for selecting the interpulse delay and pulse energy in the range from 50mJ to 200mJ. The laser pulse repetition rate is 10 Hz, and a single 500 mm planoconvex BK-7 lens is used to focus the laser beam to ablate the sample.

Typical experimental setups for LIBS measurements make use of a single spectrograph, thus are inherently characterized for having either a high spectral resolution or a broad spectral range. Nonetheless in view of analytical application here we require both a high spectral resolution and a large spectral range, the first needed to deconvolute the hydrogen and tungsten interfering line from the deuterium emission, the second needed to have enough spectral emissions for reliable determination of plasma parameters used in analysis method. This aspect, which is critical for the present experiment, has been faced by setting up two optical detection systems for the simultaneous acquisition of individual DP-LIBS spectra from the same laser shot. High and low spectral resolution is achieved by two different optical assemblies; the first is a condenser-fiber assembly allowing for narrow band high resolution, while the second condenser-fiber assembly is used for broad-band low resolution measurements.

In lens-fiber configuration, a single 150 mm focal length planoconvex BK7 lens is coupled into a circular bundle end of 22 individual fused silica fibers. The lens is positioned at 300 mm from both sample and fiber bundle end for an optimized light collection. The other end of the fiber bundle is configured as a linear array and is placed in front of the entrance slit of the spectrometer (50 μm). The collected light is focused into a 0.55 m focal length Czerny–Turner spectrograph (Triax 550, Jobin–Yvon) spectrally dispersed by a 2400 grooves/mm grating with a spectral resolution of $\delta\lambda/\lambda = 15,000$. The detector is an ICCD camera (DH534-18F, Andor) with 1024×256 pixel array and covers a spectral window of 12 nm.

In condenser-fiber assembly, the optical receiver (ME-OPT-007, Andor) is placed at 35 cm from the sample; the exit of the condenser is coupled into a 50 μm fused silica fiber. The other end of the fiber is connected to the entrance port of the spectrometer. The collected light is focused into a echelle spectrometer (Mechelle 5000, Andor) and detected by an ICCD camera (DH734-18F, Andor).

This arrangement provides both the possibility of well resolving the hydrogen and its isotopes, while allowing for a better estimate of plasma parameters from the many available lines emitted from sample major constituents and spanning over the spectral range from 250 to 800 nm. In the case of the present measures a reduction of the available range is caused by collecting the plasma light through a vacuum window not specifically designed for high transmittance in the UV region (up to 350 nm). So the UV emission lines of W and Al are not available for a reliable analysis of the plasma parameters (temperature and electron density) and this analysis was performed looking at the emission lines in the VIS region of the spectrum.

The chamber containing the sample under study is connected to a vacuum system (Turbolab, Leybold); the pressure inside the analysis chamber is 10^{-5} mbar. The sample holder is mounted on a XY translator stage, so that unexposed sample surface can be faced to the ablating laser.

Result and discussion

The experiments reported in the present paper deal with Double Pulse (DP) technique, which has been reported as a viable technique to enhance the LIBS signal in several experimental conditions including the atmospheric air pressure [21] and vacuum [22]. Actually the sample was placed in a vacuum chamber with a residual pressure of 10^{-5} mbar; a careful optimization of the experimental parameters (interpulse delay, gate duration and gate delay) allowed optimum compromise between ablated mass and plasma temperature.

Interpulse delay plays an important role in DP-LIBS signal enhancement since it regulates the laser interactions with the target and the plasma, thus influencing the ablation efficiency and plasma re-heating processes. For this experiment the delay be-

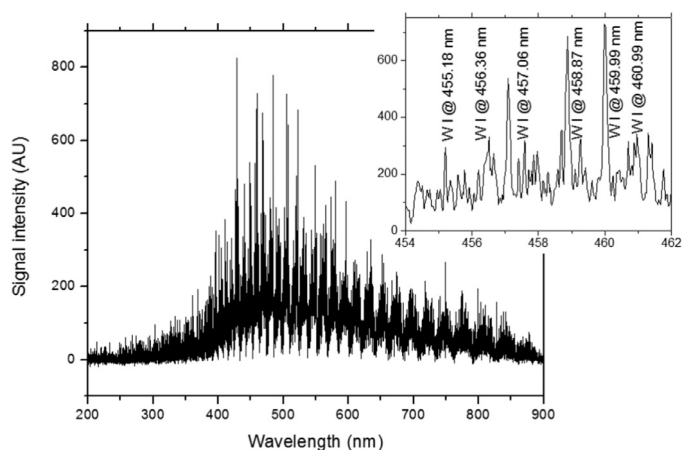


Fig. 2. Low resolution LIBS spectrum on deuterated sample with 600 ns delay and 1200 ns gate; the inset shows the 454 nm to 462 nm spectral region of interest for the tungsten emissions.

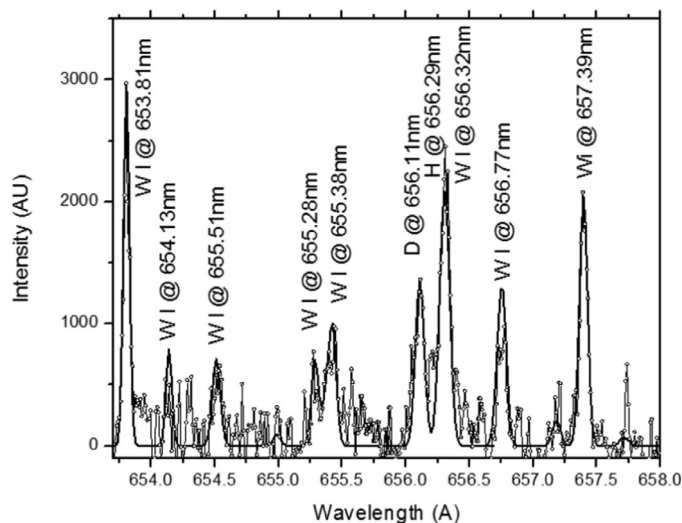


Fig. 3. High resolution LIBS spectrum on deuterated sample (dot experimental data, continuous line is a best fit); spectrum acquired with 600 ns delay and 100 ns gate.

tween the two lasers was optimized to 300 ns. Two laser pulses with the same energy content were used; nominal energy for the first pulse was 200 mJ, the same energy was also used for the second pulse, and this corresponds to an optimum value. Fig. 2 shows a typical low resolution LIBS spectrum from deuterated sample; here the spectral range is from 200 nm to 900 nm, the delay between the first laser excitation and detection was optimized at 600 ns, while the detection gate was 1200 ns. Fig. 2 also shows a UV region scarcely populated by W II emissions; this is due to the reduced transmittance of the glass vacuum window. The inset shows a large S/N (more 20 db at 460 nm) in a spectral region of interest for the tungsten emission, while not enough the spectral sensitivity and resolution is achieved for the detection of hydrogen and/or deuterium emission lines.

On the other hand, the high resolution acquisition system has much higher sensitivity; indeed the same laser shot producing the signal in Fig. 2 was also simultaneously acquired by the second system, and the spectrum is shown in Fig. 3 for the 654 nm–659 nm spectral region; in this case the detection delay was the same, while the gate duration was 100 ns which is considerably smaller than that used for the low resolution system (1200 ns); use of narrow gate with also facilitate the stationarity of the detected

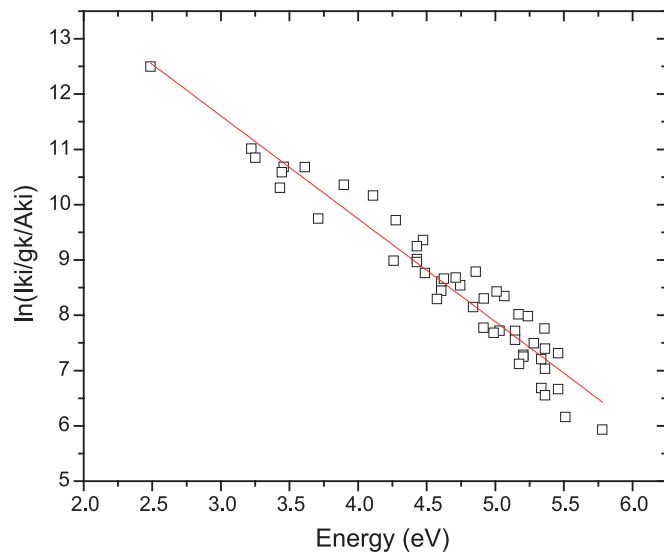


Fig. 4. Boltzmann plot of DP-LIBS at interpulse delay of 300 ns and gate delay 600 ns from the first laser excitation.

emission, reducing problems connected with N_e and T_e time dependence.

In Fig. 3 the experimental data are represented by dot, while a continuous line is a best fit

Actual experimentation showed the simultaneous presence in the LIBS spectra of H and D lines, where the hydrogen contribution is due to contamination with sample exposure to the environment at atmospheric pressure. Previous study in a reduced atmosphere following the time dynamic of the relative contribution of H and D showed a segregation of the deuterium [23]. This effect, which is especially relevant in vacuum where the plume expansion is more pronounced, is consistent with a mass-dependent expansion dynamics and for double pulse experiment suggests the use of relatively large gate delay to enhance the sensitivity and favor the analytical determination of deuterium.

Plasma temperature (T_e) was determined using the Boltzmann plot and assuming LTE conditions. Each LIBS spectrum is obtained from a single laser shot and the experimental line intensity corrected for the spectral efficiency and normalized to the degeneracy and level lifetime was plotted against the energy of upper level for each transition. Fig. 4 shows the Boltzmann plot obtained on the examined sample after the optimization of experimental conditions; the selected analytical lines form a superset of the critical selection made by Lissovski [20]. The temperature is then calculated by using straight-line approximation fit to the data, where the slope of the line is equal to $-1/kT$; the resulting estimate for the temperature is $T = 6500 \pm 250$ K.

The electron density was derived from the analysis of Stark broadened spectral line profile of the D_α line at 656.1 nm. Use of that line has several significant practical advantages since it is optically thin and has a relatively large Lorentzian broadening, thus ensuring a small error in electron density computation.

The theoretical Stark broadening of the D_α line is obtained by modifying the approximation of Gigosos [24] to account for the fact that in the range of electron density between 10^{15} and 10^{17} cm^{-3} the experimental Stark broadening of Balmer alpha line of deuterium line is approximately 10% smaller than the corresponding line width of hydrogen [25]. The equation relating the electron density to the line full width at half area (FWHA) is obtained by using a modified version of the Gigosos broadening coefficient and reads as:

$$N_e = 10^{17} (\Delta\lambda_{FWHA}/0.499)^{1.4713} \quad (1)$$

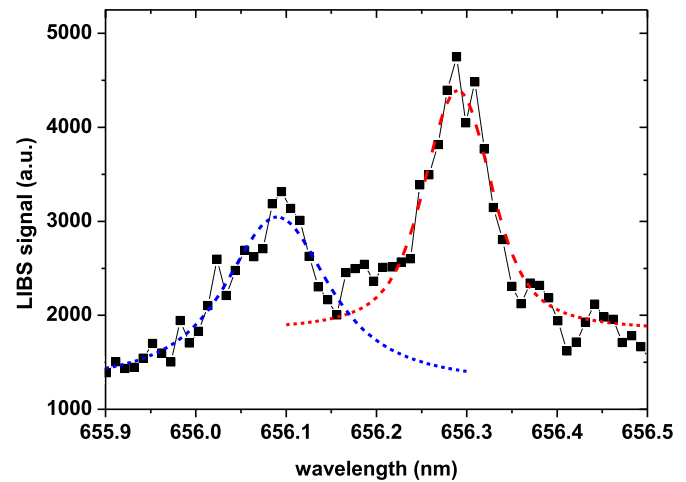


Fig. 5. Experimental data (square dot) and Voigt profile (dashed line) of the D_α emission at 656.1 nm.

where N_e is in cm^{-3} units and the $\Delta\lambda_{FWHA}$ is expressed in nm.

Line profile of D_α line was recorded with the high resolution Czerny–Turner spectrograph, then the experimental line profile was fitted with a Voigt profile; here the gaussian contribution accounts for the instrumental and the Doppler broadening, whereas the lorentzian contribution accounts for the natural and Stark broadening.

The instrumental broadening, evaluated from the low pressure glow discharge lamp (Ne I emission at 650.65 nm Oriel 6032), was found to be ~ 0.030 nm, while the Doppler broadening at $T = 6500$ K, is evaluated to be ~ 0.032 nm. The overall gaussian broadening, estimated as the result of the convolution of instrumental and Doppler contributions, is given by [26]

$$FWHM_{\text{gaussian}} = (FWHM_{\text{instr}}^2 + FWHM_{\text{Doppler}}^2)^{1/2} = 0.044 \text{ nm} \quad (2)$$

The gaussian broadening is then inserted as a constant parameter in the Voigt fitting function and the lorentzian contribution was computed by best fitting the theoretical profile with the experimental lineshape (see Fig. 5).

The lorentzian broadening was about 0.13 ± 0.06 nm, while the density was $N_e = (1.3 \pm 0.6) \times 10^{16} \text{ cm}^{-3}$. This value is numerically consistent with the electron density value obtained using the approximation accounting for ion and electron broadening computed by using the fractional intensity width of hydrogen tabulated by Griem [27].

The temperature and the electron density function of the gate delay are shown in Fig. 6; for delay time ranging from 600 ns to 1000 ns the electron number density varied from 0.6×10^{16} to $1.4 \times 10^{16} \text{ cm}^{-3}$, while at shorter gate delay the too large interference between the H_α and D_α lines prevents an accurate N_e computation.

A necessary condition for the LTE assumption is the McWhirter criterion, giving the lower limit for the electron number density to maintain the energy level populations to within 10% of Boltzmann equilibrium, while competing with radiative processes. Evaluation for the W I transition at 429.46 nm, $\Delta E = 3$ eV, and at the highest temperature in this study, the lower limit for N_e is $3.5 \times 10^{15} \text{ cm}^{-3}$, which is lower than the value deduced from Stark broadening. Although the satisfaction of the McWhirter criterion is not a sufficient condition, the existence of LTE is assumed in the following. In conclusion Fig. 6 shows that in all the tested experimental conditions the laser produced plasma complies with the requirements of the McWhirter criterion; however the optimal condition was found at 600 ns gate delay since the LTE condition is reached

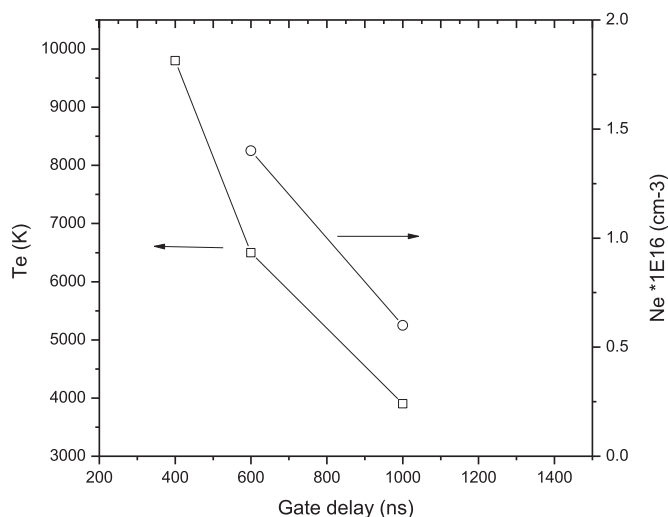


Fig. 6. Electron temperature (left scale) and density (right scale) for DP-LIBS experiment versus gate delay computed from the first laser pulse.

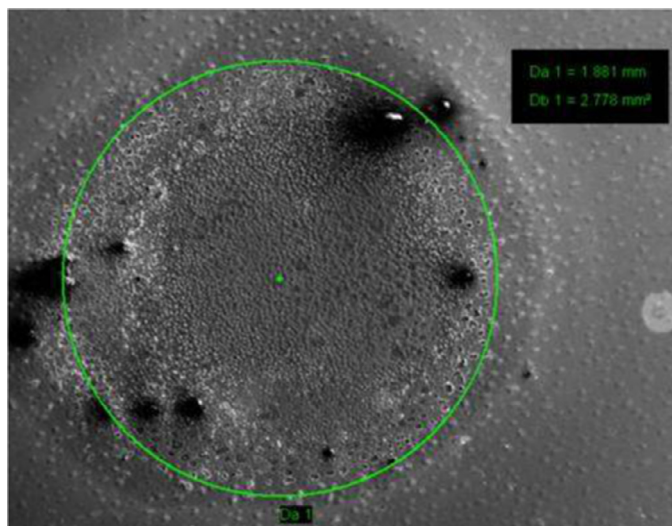


Fig. 7. SEM image of crater produced by DP-LIBS; for this particular case one couple of laser pulses of 200 + 200 mJ each was used, with 300 ns interpulse delay.

and the spectrum is still high enough for the identification of the low weaker W I line emission.

To estimate the power density delivered to the sample, superficial analysis by SEM is presented. The crater produced by a single laser shot in double pulse regime is presented in Fig. 7. As can be seen the crater size has a circular shape; besides crater formation, thermal effects produce damage and melting fragment are visible on the border. Considering thermal effects as part of the superficial sample destruction, the irradiated area extends over a circular region of approximately 1800 μm of diameter. For this particular example the ablative pulses of 200 + 200 mJ resulted in a power density of 1.8 GW/cm^2 ; it must be noted however that the laser energy effectively coupled with the target can be substantially less since the plasma generated from the first laser pulse effectively shields the second laser pulse. This mechanism strongly depends on the inter-pulse delay which dictates the laser interactions with the plasma and influences the ablation efficiency. Finally we observe that the measured power density is consistent with a stoichiometric ablation of the sample, thus satisfying a basic assumption of DP-LIBS.

Application of the CF method to the sample under study gives a deuterium content concentration of 1.3 \pm 0.2% at units. It is worth to note that the error on the concentration here reported could be underestimated since only the uncertainties from error propagation were considered. Although important, the influence of the statistical error affecting the line intensities was not included in the error computation because no more than a few laser shot were allowed on the available sample. The D concentration can be compared with the one measured with Nuclear Reaction Analysis (NRA) on a tungsten sample implanted in Pilot-PSI with similar deuterium fluence [28]. In that experiment a polycrystalline tungsten target was implanted with 40 eV deuterium flux of $1.0 \times 10^{24} \text{ m}^{-2}\text{s}^{-1}$ for 750 s, resulting in a fluence of $0.8 \times 10^{27} \text{ m}^{-2}$. The concentration of D as measured by NRA was maximum at the near surface and equal to 1% at; taking into account the different kind of tungsten sample (tungsten bulk and tungsten coating on molybdenum substrate) the obtained result is in satisfactory agreement with LIBS measurements.

Based on previous estimates of the ablation efficiency, the mass removal is in the order of 20–40 μg . It is worth noticing that the assessment of the ablated material paves the way to a quantitative estimate of the total amount of deuterium contained in the sample, once the relative contribution of deuterium is known from the CF analysis.

Conclusions

The combination of DP-LIBS and Calibration Free analysis has been used for quantitative analysis of deuterium. Relatively high ablative energies densities produced limited thermal effect, and assured for stoichiometric ablation; the results obtained in the present experiments indicate the possibility to perform deuterium quantitative determination, and the same technique can also be applied for the quantification of tritium. The changes in the environment produced by double plasma excitation, demonstrate that the DP technique is an effective method for LIBS signal enhancement. In this case, the plasma produced by the second laser pulse together with the reheating of the plasma produced by the first laser, lead to an increase of density particles and of the collision rates which contribute to populate higher energy states in the atoms and consequently to an enhancement of the emission intensity.

Changing the surrounding environment of plasmas is a potential method for improving LIBS sensitivity which eventually can be combined with other enhancing effects such as magnetic field present in fusion machines without adding any design complexity.

The matrix effect and the problems related to the surface contaminants expected in fusion machines has overcome by using the calibration free technique; moreover, it is worth mention that the approach here presented to determine the concentration of minor constituents shows an accuracy of the order of 20%, which is within the requirement put forward by fusion machines as for example ITER.

Acknowledgments

This work has been carried out within the framework of the EUROfusion Consortium and has received funding from the Euratom research and training programme 2014–2018 under grant agreement No 633053. The views and opinions expressed herein do not necessarily reflect those of the European Commission.

References

- [1] I.R. Cristescu, I. Cristescu, L. Doerr, M. Glugla, D. Murdoch, Tritium inventories and tritium safety design principles for the fuel cycle of ITER, *Nucl. Fusion* 47 (2007) S458–S463.

- [2] J. Roth, E. Tsitrone, T. Loarer, V. Philipps, S. Brezinsek, A. Loarte, G.F. Counsell, R.P. Doerner, K. Schmid, O.V. Ogorodnikova, R.A. Causey, Tritium inventory in ITER plasma-facing materials and tritium removal procedures, *Plasma Phys. Control. Fusion* 50 (2008) 103001.
- [3] E. Tognoni, V. Palleschi, M. Corsi, G. Cristoforetti, *Spectrochim. Acta Part B* 57 (2002) 1115.
- [4] R.E. Neuhauser, U. Panne, R. Niessner, Laser-induced plasma spectroscopy, *Anal. Chem. Acta* 392 (1999) 47–54.
- [5] R.E. Russo, *Laser Ablation, Appl. Spectrosc.* 49 (1995) 14.
- [6] A. Lissovskia, K. Piip, L. Hämarik, M. Aints, M. Laan, P. Paris, A. Hakola, J. Karhunen, LIBS for tungsten diagnostics in vacuum: selection of analytes, *JNM* 463 (2015) 923–926.
- [7] W. Zhenzhen Wang, Y. Deguchi, J. Yan, J. Liu, Comparison of the detection characteristics of trace species using laser-induced breakdown spectroscopy and laser breakdown time-of-flight mass spectrometry, *Sensors* 15 (2015) 5982–6008.
- [8] G. Cristoforetti, S. Legnaioli, V. Palleschi, A. Salvetti, E. Tognoni, *Appl. Phys. B* 80 (2005) 559.
- [9] M. Capitelli, F. Capitelli, A. Eletsii, *Spectrochim. Acta Part B* 55 (2000) 559–574.
- [10] M. Capitelli, G. Colonna, M. Catella, F. Capitelli, A. Eletsii, *Chem. Phys. Lett.* 316 (2000) 517.
- [11] E. Tognoni, G. Cristoforetti, S. Legnaioli, V. Palleschi, A. Salvetti, M. Mueller, U. Panne, I. Gornushkin, *Spectrochim. Acta, Part B* 62 (2007) 1287.
- [12] A. Malaquias, V. Phillips, A. Huber, A. Hakola, J. Likonen, J. Kolehmainen, S. Tervakangas, M. Aints, P. Paris, M. Laan, A. Lissovski, S. Almaviva, L. Caneve, F. Colao, G. Maddaluno, M. Kubkowska, P. Gasior, H. Meiden, A. Lof, P. Zeijmans, et al., Development of ITER relevant laser techniques for deposited layer characterisation and tritium inventory, *J. Nuclear Mater.* 438 (2013) S936–S939.
- [13] A. Semerok, D.L. Hermite, J.M. Weulersse, J.L. Lacour, G. Cheymol, M. Kempenaars, N. Bekris, C. Grisolia, Laser induced breakdown spectroscopy application in joint European torus, *Spectrochim. Acta Part B* 123 (2016) 121–128.
- [14] N. Gierse, S. Brezinsek, J.W. Coenen, T.F. Giesen, A. Huber, M. Laengner, S. Moller, M. Nonhoff, V. Philipps, A. Pospieszczyk, B. Schweer, G. Sergienko, Q. Xiao, M. Zlobinski, U. Samm, In situ deuterium inventory measurements of a-C:D layers on tungsten in TEXTOR by laser induced ablation spectroscopy, *Phys. Scr.* T159 (2014) 014054.
- [15] K. Piip, G. De Temmerman, H.J. van der Meiden, H. Mändar, LIBS analysis of tungsten coatings exposed to Magnum PSI ELM-like plasma, *J. Nuclear Mater.* 463 (2015) 919–922.
- [16] M. Pribula, J. Kristof, M. Suchonova, M. Hornackova, J. Plavcan, A. Hakola, P. Veis, Use of the near vacuum UV spectral range for the analysis of W-based materials for fusion applications using LIBS, *Phys. Scri.* T167 (2016) 014045.
- [17] J. Butikova, A. Sarakovskis, I. Tale, Laser Induced Plasma Spectroscopy of plasma facing materials, 35th EPS Conference on Plasma Phys. Hersonissos, 9 - 13 June 2008 ECA, 2008 Vol.32D, P-2.011.
- [18] F. Rezaei, P. Karimi, S.H. Tavassoli, Effect of self-absorption correction on LIBS measurements by calibration curve and artificial neural network, *Appl. Phys. B* 114 (2014) 591–600.
- [19] H.E. Bauer, F. Leis, K. Niemax, *Spectrochim. Acta Part B* 53 (1998) 1815–1825.
- [20] A. Lissovski, K. Piip, L. Hamarik, M. Aints, M. Laan, P. Paris, A. Hakola, J. Karhunen, LIBS for tungsten diagnostics in vacuum: selection of analytes, *J. Nuclear Mater.* 463 (2015) 923–926.
- [21] V.I. Babushok, F.C. DeLucia Jr., J.L. Gottfried, C.A. Munson, A.W. Miziolek, Double pulse laser ablation and plasma: laser induced breakdown spectroscopy signal enhancement, *Spectrochim. Acta B* 61 (2006) 999–1014.
- [22] T. Donnelly, J.G. Lunney, S. Amoroso, R. Bruzzese, X. Wang, X. Ni, Double pulse ultrafast laser ablation of nickel in vacuum, *J. Appl. Phys.* 106 (2009) 1–5.
- [23] L. Mercadier, J. Hermann, C. Grisolia, A. Semerok, Plume segregation observed in hydrogen and deuterium containing plasmas produced by laser ablation of carbon fiber tiles from a fusion reactor, *Spectrochim. Acta Part B* 65 (2010) 715–720.
- [24] M.A. Gigosos, M.A. Gonzalez, V. Cardenoso, *Spectrochimica acta B* 58 (2003) 1489–1504.
- [25] H. Ehrich, Experimental study of Balmer- α Stark broadening, *Z. Naturforsch.* 34a (1979) 188–191.
- [26] H.J. Kunze, *Introduction to Plasma Spectroscopy*, Springer, Berlin-Heidelberg, 2009.
- [27] H.R. Griem, *Spectral Line Broadening By Plasmas*, Academic Press, New York, 1974.
- [28] M.H.J. Hoen, Surface morphology and deuterium retention of tungsten after low- and high-ux deuterium plasma exposure, *Nucl. Fusion* (2016).